

Temperature-dependent charge transport in the compensated ferrimagnet $\text{Mn}_{1.5}\text{V}_{0.5}\text{FeAl}$ from first principles

R. Stinshoff,¹ S. Wimmer,² H. Ebert,² G. H. Fecher,¹ C. Felser,¹ and S. Chadov¹

¹*Max-Planck-Institut für Chemische Physik fester Stoffe, 01187 Dresden, Germany*

²*Ludwig-Maximilians-Universität, Dept. Chemie, Butenandtstr. 11, 81377 München, Germany*

We present an *ab-initio* study of the temperature-dependent longitudinal and anomalous Hall resistivities in the compensated collinear ferrimagnet $\text{Mn}_{1.5}\text{V}_{0.5}\text{FeAl}$. Its transport properties are calculated using the general fully relativistic Kubo–Bastin formalism and their temperature dependency is accounted for magnetic and structural disorder. Both scattering sources, together with the residual chemical disorder, were treated equally provided by the CPA (Coherent Potential Approximation) SPR-KKR (Spin-Polarized Relativistic Korringa-Kohn-Rostoker) method. All calculated properties showed good agreement with a recent experimental results, providing useful specific information on the chemical and magnetic arrangement as well as on the influence of disorder. Finally, we demonstrated that the anomalous Hall effect in such compensated systems occurs regardless of the vanishing net spin moment.

PACS numbers: 75.50.Gg, 72.80.Ng, 85.30.Fg

Keywords: compensated ferrimagnets, conductivity, anomalous Hall effect, disorder

Magnetically compensated systems provide an attractive base for the next generation of spintronic devices [1]. Their investigation is motivated by potential applications in various technological fields, such as new types of RAM, detectors, microscopic tips, etc, in which the interest is focused on an alternative manipulation of spins, absence of stray fields and higher operating frequencies. Magnetically compensated systems have different order parameters than ferromagnets, such as staggered magnetization [2, 3] or magnetic chirality [4–6], which can be manipulated and detected by either magnetic fields or pulsed electric currents. However, the absence of net magnetization does not exclude the possibility that such materials will exhibit the anomalous Hall effect (AHE) [7], Kerr effect [8] or high spin-polarization [9–11]. For example, in case of the planar noncollinear antiferromagnets (e.g., Mn_3Ir) AHE has been predicted [12] for the case when the mirror symmetry is broken. By considering magnetic compensation in the cubic ferrimagnets, it is important to note that, both typical cubic structures with $Fm\bar{3}m$ or $F\bar{4}3m$ space groups correspond to $I\bar{4}/mm'm'$ or $I\bar{4}m'2'$ magnetic space groups, respectively. Both cases belong to the magnetic Laue group $4/mmm'$ [13, 14] which leads to the following shape of the conductivity tensor:

$$\underline{\sigma} = \begin{pmatrix} \sigma_{xx} & \sigma_H & 0 \\ -\sigma_H & \sigma_{xx} & 0 \\ 0 & 0 & \sigma_{zz} \end{pmatrix}, \quad (1)$$

where σ_H is the anomalous Hall component. Obviously, σ_H will have a non-vanishing amplitude if there is a difference between the spin-up and -down projections of the electronic structure, which can be fulfilled if the magnetic moment of one atom type is compensated by the antiparallel moments from the other atom types. It is particularly easy to realize such systems using cubic Heusler alloys since most of them obey

the Slater–Pauling rule [15, 16], suggesting that compensated ferrimagnets can be found among compounds having 24 electron formula units. Some compensated Heusler ferrimagnets have been already reported, such as $\text{MnCo}_{4/3}\text{Ga}_{5/3}$ [17]. Ferrimagnetic compensation can also be induced in the tetragonal structures [18], e.g., in the case of $\text{Mn}_{1.4}\text{Pt}_{0.6}\text{Ga}$ [19]; however, the deviation from the Slater–Pauling rule does not allow for a clear recipe for the exact compensating stoichiometry.

The first experimental evidence of non-zero AHE in compensated cubic ferrimagnets was given recently [20, 21] for the Heusler compound $\text{Mn}_{1.5}\text{V}_{0.5}\text{FeAl}$. Additional calculations [21] have shown that this system is half-metallic in agreement with the Slater–Pauling rule, indicating that the observed AHE is due to the aforementioned strong asymmetry of the spin-channels. Here, we investigate this scenario by first-principles calculations on the system $\text{Mn}_{1.5}\text{V}_{0.5}\text{FeAl}$ and verify that the experimental non-zero AHE is an intrinsic property of the compensated ferrimagnets, rather than a consequence of the small remaining magnetization induced by deviations from stoichiometry. We employed the fully-relativistic SPR-KKR (Spin-Polarized Relativistic Korringa-Kohn-Rostoker) method using the standard generalized gradient approximation [22] for the exchange-correlation potential. The structural information on $\text{Mn}_{1.5}\text{V}_{0.5}\text{FeAl}$ is taken from a recent experiment [20].

Though the origins of AHE being well understood theoretically, a realistic combined first-principles description still remains a challenging computational task. At present, the most general approach for equally considering the sources of AHE is the so-called Kubo–Bastin formalism. Being implemented within the SPR-KKR method [23, 24], it allows us to deal with the charge transport in solids by treating various disorder effects on the basis of the CPA (Coherent Potential Approxima-

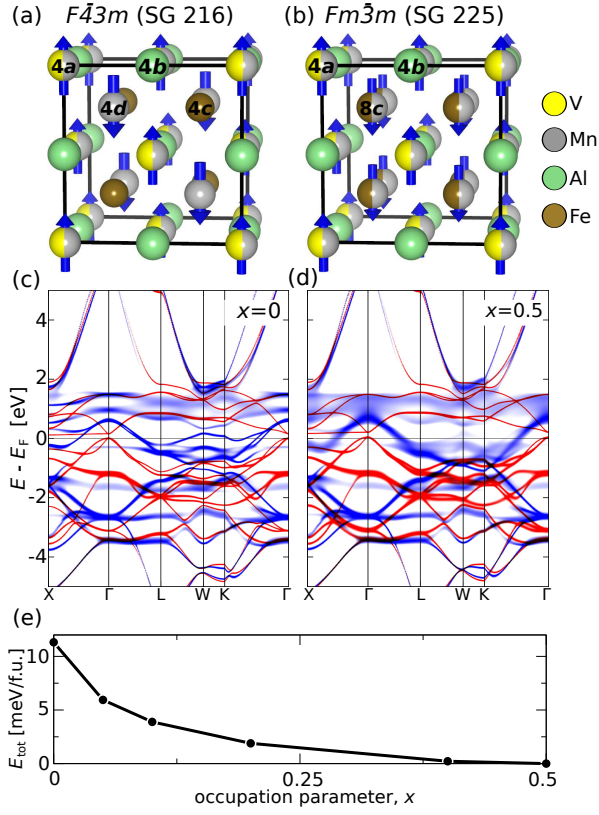


FIG. 1: $\text{Mn}_{1.5}\text{V}_{0.5}\text{FeAl}$ within (a) $F\bar{4}3m$ (SG 216, with 4c and 4d Wyckoff sites occupied by Mn and Fe, respectively) and (b) $Fm\bar{3}m$ (SG 225, for which 4c and 4d sites become equivalent by changing to common type 8c with random $\text{Mn}_{0.5}\text{Fe}_{0.5}$ occupation). Other sites, 4a and 4b, occupied by $\text{Mn}_{0.5}\text{V}_{0.5}$ and Al, respectively, remain the same in both structures. Arrows indicate the spin moments of Mn atoms. (c) and (d) show the corresponding (to (a) and (b), respectively) spin-resolved (red - spin-up, blue - spin-down) spectral densities. (e) The total energy as a function of x (occupation parameter), i.e., the amount of Mn in 4d position: $x = 0$ corresponds to (a), $x = 0.5$ - to (b).

tion) [25, 26].

Since the X-ray diffraction (XRD) refinement [20] does not unambiguously resolve the occupancies of the 4c and 4d Wyckoff positions, we first specified the chemical order in the system. Most of the integral characteristics of the system, such as the magnetization, are not very sensitive to the partial ordering; however partial ordering might significantly influence the charge transport. Treating our system within the $F\bar{4}3m$ symmetry, we assumed 4c and 4d sites were different. This allowed us to mix Mn with Fe, gradually going from the most ordered case $(\text{Mn})_{4d}(\text{Fe})_{4c}$ ($F\bar{4}3m$) to the most disordered case $(\text{Mn}_{0.5}\text{Fe}_{0.5})_{4d}(\text{Mn}_{0.5}\text{Fe}_{0.5})_{4c}$, which has higher effective symmetry ($Fm\bar{3}m$). Both variants are shown in Fig. 1 a and b. Even though their electronic structures (Fig. 1 c, d) were looking similar, increased broadening of the spin-down states was observed in the vicinity of the

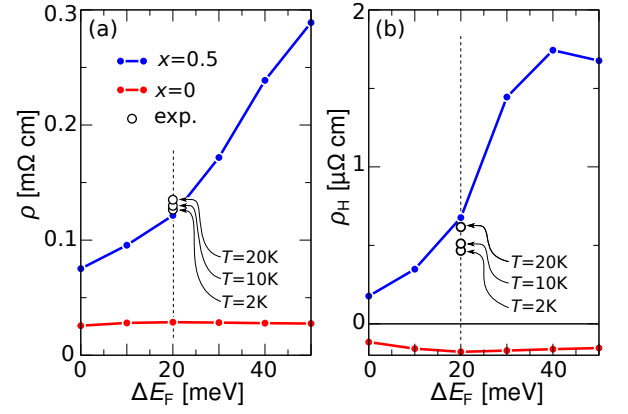


FIG. 2: Residual resistivities as a function of the Fermi energy shift $\Delta E_F = E'_F - E_F$. (a) Longitudinal resistivity ρ , (b) anomalous Hall resistivity ρ_H . Red and blue curves correspond to the $x = 0$ and $x = 0.5$ variants; empty circles are the experimental values [21] measured at low temperatures (indicated explicitly).

Fermi energy E_F for the case (d), which was caused by the additional Mn/Fe disorder. This broadening should impose a drastic difference in the transport properties of the case (d) with respect to case (c). Calculating the total energy as a function of the occupation rate x : $(\text{Mn}_x\text{Fe}_{1-x})_{4d}(\text{Mn}_{1-x}\text{Fe}_x)_{4c}$, $0 \leq x \leq 0.5$, provided information concerning the most stable phase. As shown in Fig. 1 e, the total energy decreased monotonically with x and reached its minimum at $x = 0.5$. This behavior indicates that $\text{Mn}_{1.5}\text{V}_{0.5}\text{FeAl}$ effectively has $Fm\bar{3}m$ symmetry.

Having specified the chemical order, we proceeded with the precise calibration of the Fermi energy E_F . Again, small deviations of E_F do not influence the integral properties as the magnetization, but might be crucial for the transport properties. These deviations can occur both in experiment (e.g., due to chemical and structural imperfections) as well as in calculations (e.g., due to the spherical approximation of the atomic potentials). For this reason, we computed both $\rho = 1/3 \cdot (2\rho_{xx} + \rho_{zz})$ and $\rho_H = \rho_{xy}$ as functions of the E_F position (Fig. 2). For $x = 0.5$ we observed a strong dependence on E_F for both ρ and ρ_H , which showed the best simultaneous agreement with experiment at ~ 20 meV above the nominal E_F . At the same time, for $x = 0$ both quantities strongly deviated from experiment within the whole range of ΔE_F .

The temperature dependency of the charge transport for $x = 0.5$ was examined by considering two basic sources of disorder induced by temperature: phonons and magnons. Here they are considered in an approximate way as an additional quasi-static disorder: phonons - as positional disorder, magnons - as spin-orientation disorder [27]. In addition, we neglected the T -dependency of the Fermi-Dirac statistics and identified the actual chemical potential $\mu(T)$ with E_F . The ability to treat

both thermal disorder sources within the CPA formalism made this approach especially convenient. Even though the non-local details and the specific features of the thermal oscillatory modes are neglected, the practical use of this approach has been convincingly demonstrated [27–29].

The T -dependency of the mean amplitude of the atomic displacements was determined here by the Debye theory (the effective Debye temperature was taken as an average over atomic types), whereas the directions of displacements were selected along the basis vectors to keep the conformity with the lattice. The atomic spins were assumed to have T -independent amplitudes m_i ($i = 1, \dots, N$; N is the number of atoms in the unit cell), and thus were calculated from first principles, but the adequateness of the T -dependency of their angular distribution expressed by weights, must be determined. At a fixed temperature T , the angular distribution of the i -th atomic spin gives its effective average value: $m_i \sum_{\nu} p_{i\nu}(T) \vec{e}_{\nu} = \langle \vec{m}_i \rangle(T)$ ($\{\vec{e}_{\nu}\}$ is a fixed set of all possible spatial directions). The angular distribution was assumed to be Gibbs-like (see Eqs. 13-15 in Ref. [27]) with weights $\{p_{i\nu}(T)\}$ determined by fitting the experimental value: $\langle \vec{m}_i \rangle(T) = \vec{m}_i^{\text{exp}}(T)$. Such a mapping is unique only for a single magnetic sublattice, where the experimental magnetization unambiguously defines the angular distribution of each atomic spin, since $\forall i: m_{iz}^{\text{exp}} = M_{\text{exp}}/N$ (index “z” denotes a projection on the common magnetization axis). In the present case, even though $M_{\text{exp}}(T)$ is known, the unit cell contains five different magnetic sublattices: $i = \text{V}(4a)$, $\text{Mn}(4a)$, $\text{V}(4b)$, $\text{Fe}(8c)$ and $\text{Mn}(8c)$. We simplified this situation by assuming that the same form of the T -dependency applies to all atomic spins that randomly share the same Wyckoff site, which reduced the number of magnetic sublattices from five to three (i.e., $i = 4a$, $4b$ and $8c$). To avoid the remaining ambiguity, we assumed some reasonable form of the T -dependency for each sublattice, e.g., by implying a sublattice-specific Bloch’s law: $\langle m_{iz} \rangle(T) = m_{iz} (1 - (T/T_i)^{\alpha_i})^{\beta_i}$, where α_i , β_i and T_i (playing the role of an ordering temperature for the i -th sublattice) are T -independent fitting parameters and $m_{iz} = m_{iz}(0)$ - the ground-state atomic spin moments calculated from first principles. Thus, we fitted $M_{\text{exp}}(T)$ by using the following expression: $\sum_i m_{iz} (1 - (T/T_i)^{\alpha_i})^{\beta_i} = M_{\text{fit}}(T) \rightarrow M_{\text{exp}}(T)$, with i running over three atomic sublattices entering the unit cell with the corresponding multiplicities, which are implicitly included in m_{iz} . The fit (see Fig.3) resulted in rather close sets for the ordering temperatures $T_i = 345.6, 345.0$ and 345.0K , as well as for the power factors $\alpha_i = 2.52, 2.92$ and 3.10 , $\beta_i = 0.56, 0.35$ and 0.55 for sites $4a$, $4b$ and $8c$, respectively. These factors appeared to have the same order of magnitude as those in the conventional Bloch’s law ($\alpha = 3/2, \beta = 1/3$).

The conductivities σ and σ_{H} calculated as functions of

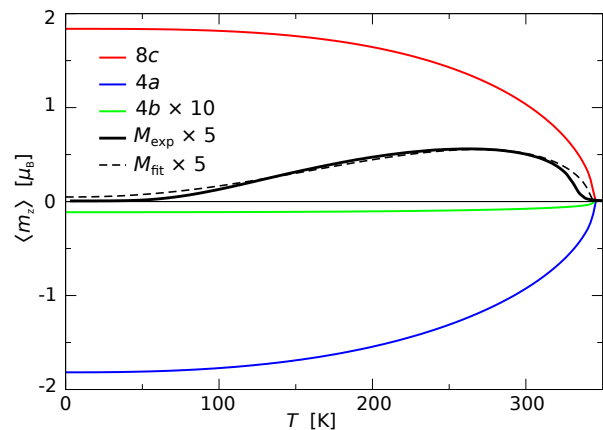


FIG. 3: Experimental magnetization [21] in $\mu_B/\text{f.u.}$ (black solid line) versus fit (black dashed line) together with the z-projections of the sublattice spin moments derived from the fit (red, blue and green correspond to $8c$ ($\text{Mn}_{0.5}\text{Fe}_{0.5}$), $4a$ ($\text{Mn}_{0.5}\text{V}_{0.5}$) and $4b$ (Al), respectively).

T are shown in Fig.4. The effects of spin-fluctuations and atomic vibrations are demonstrated by two additional curves, where the calculation accounts either only for spin-fluctuations (marked as “fluct.”) or only for atomic vibrations (“vib.”). These scattering sources cannot be combined, neither as parallel nor as sequential resistors (i.e., neither of these combinations gives the blue curve), even at low temperatures. On the other hand, the result based on the spin-fluctuations alone (green) followed the total curve (blue) more closely indicating that the spin disorder is the dominant scattering source. Both computed σ and σ_{H} reasonably agreed with the experimental values over the whole temperature range. The strongest deviation from experiment was simultaneously observed around 100K for both quantities (in case of $\sigma_{\text{H}}@100\text{K}$ the deviation was more than 50%, however due to $\sigma_{\text{H}}/\sigma \sim 10^{-3}$, for the absolute deviation the relation $\delta\sigma_{\text{H}} \sim \sigma_{\text{H}} \ll \delta\sigma \ll \sigma$ holds). The main reason for the deviations are the aforementioned assumptions about the angular distribution of the spin moments, which might deviate from the actual distribution more strongly in the T -range where the dispersion is already large, but the distribution is still far from uniform. The adequate description of this temperature regime becomes rather complicated, but it can be improved by systematically considering different aspects influencing the distribution of the local moments, such as the specific features of the magnon dispersion, additional angular correlations imposed by relativistic effects, and possible longitudinal spin fluctuations.

In addition to the determination of the chemical order, the present calculations explain several aspects specific to ferrimagnets, such as the directions of local moments in the magnetically compensated state. Since the reversal of local moment occurs simultaneously with the sign change

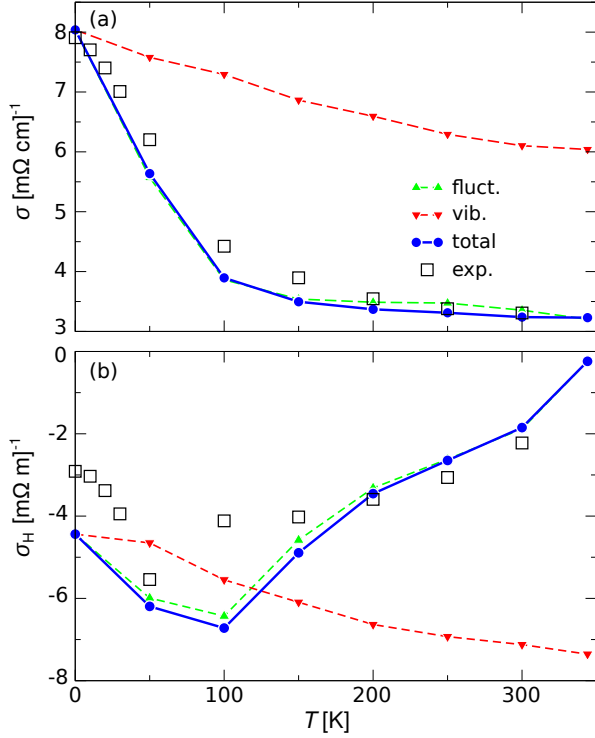


FIG. 4: (a) Longitudinal σ and (b) anomalous Hall σ_H conductivities. Dashed green (up-triangles) and red (down-triangles) curves correspond to the case when only either magnetic fluctuation or atomic vibrations, respectively, are taken into account. The blue curve (circles) corresponds to the simultaneous inclusion of both scattering sources. Hollow squares stand for experimental values [21].

of σ_H , $\sigma_H < 0$, the moments of Mn and Fe on $8c$ positions are positive (aligned along an infinitesimal small external magnetic field), whereas those of Mn and V on $4a$ are negative. Further, the residual chemical disorder is shown to reduce the AHE: in the Kubo–Bastin formalism [24], the transverse conductivity is the sum of the Fermi-surface term (σ^I , the contribution from the conducting electrons at E_F) and the Fermi-sea term (σ^II , the contribution from the occupied states), $\sigma_H = \sigma^I + \sigma^II \sim -10^{-5} (\mu\Omega \text{ cm})^{-1}$, which appear to be large quantities with opposite sign: $\sigma^I \sim -\sigma^II \sim 5 \cdot 10^{-3} (\mu\Omega \text{ cm})^{-1}$. This relation holds in the whole temperature range up to the magnetic critical point, where both terms simultaneously vanish (see Fig. 5 a). While σ^II is almost insensitive to the residual disorder, σ^I is strongly dependent on disorder and vanishes only close to the perfect limit, thereby increasing the total sum σ_H . However, this does not apply to the present material as it is strongly disordered.

The non-trivial observation in which the ideally compensated collinear ferrimagnet can exhibit a non-zero AHE does not unambiguously follow from the above data since neither the experimental nor the theoretical situations are ideal. Small residual magnetization is present both in experiment and in

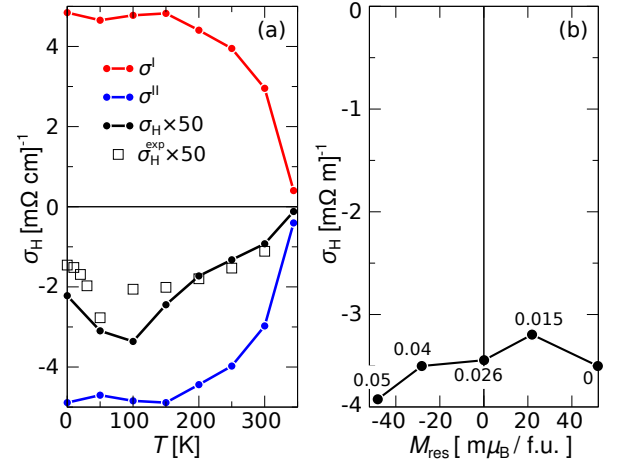


FIG. 5: (a) Anomalous Hall conductivities versus temperature. Red and blue curves correspond to the Fermi-surface σ^I and Fermi-sea σ^II terms. The black solid line is their sum σ_H , scaled up by a factor 50, as well as the experimental values [21] (σ_H^{exp} , hollow squares). (b) σ_H vs residual magnetization M_{res} . Annotated values correspond to the stoichiometric variation δ on $4a$ site, $\text{Mn}_{0.5+\delta}\text{V}_{0.5-\delta}$, which controls M_{res} .

the ground-state calculations; the computed value is $M_{\text{res}} = M_{\text{spin}} + M_{\text{orbital}} = 0.0097 + 0.0421 = 0.05 \mu_B / \text{f.u.}$ for the nominal (non-shifted) E_F . The applied calibration shift $\Delta E_F = 20 \text{ meV}$ slightly influences M_{res} further. To demonstrate the nonzero AHE at $M = 0$, we have adjusted the stoichiometry so that $M_{\text{res}} = 0$ within the numerical precision (see Fig. 5 b). This can be achieved, for instance, by a slight excess of Mn on the $4a$ site: $\text{Mn}_{0.5+\delta}\text{V}_{0.5-\delta}$. Some non-zero values of M_{res} are negative since we do not change the directions of the atomic moments, in order to preserve the sign of σ_H . As it follows, σ_H continuously changes with M_{res} and does not show any minimum in the amplitude by approaching $M_{\text{res}} = 0$. Thus, the AHE should not vanish in the ferrimagnets because of magnetic compensation. We emphasize that the aspect of full compensation is rather fundamentally than technologically relevant, since it is almost impossible in practice to remove small rest of the magnetization even in antiferromagnets. On the other hand, this makes the verification of a non-vanishing AHE technically difficult, since σ_H (or ρ_H) changes its sign with the reversal of the external magnetic field and thus passes through zero [20, 30].

To conclude, we provided an extended first-principles description of the temperature-dependent charge transport in the compensated ferrimagnet $\text{Mn}_{1.5}\text{V}_{0.5}\text{FeAl}$, which was in good agreement with experiment. In particular, we analyzed the influence of disorder on a charge transport and proved the possibility of a non-zero anomalous Hall effect in the ideally compensated state.

-
- [1] A. H. MacDonald and M. Tsoi, *Phil. Trans. R. Soc. A* **369**, 3098 (2011).
- [2] V. M. T. S. Barthem, C. V. Colin, H. Mayaffre, M.-H. Julien, and D. Givord, *Nat. Commun.* **4**, 2892 (2013).
- [3] P. Wadley, B. Howells, J. Železný, C. Andrews, V. Hills, R. P. Campion, V. Novák, K. Olejník, F. Maccherozzi, S. S. Dhesi, et al., *Science* **351**, 192404 (2016).
- [4] E. van der Bijl, R. E. Troncoso, and R. A. Duine, *Phys. Rev. B* **88**, 064417 (2013).
- [5] H. Watanabe, K. Hoshi, and J.-I. Ohe, *Phys. Rev. B* **94**, 125143 (2016).
- [6] S. Singh, S. W. D'Souza, J. Nayak, E. Suard, L. Chapon, A. Senyshyn, V. Petricek, Y. Skourski, M. Nicklas, C. Felser, et al., *Nat. Commun.* **7**, 12671 (2016).
- [7] J. Kübler and C. Felser, *Europhys. Lett.* **108**, 67001 (2014).
- [8] W. Feng, G.-Y. Guo, J. Zhou, Y. Yao, and Q. Niu, *Phys. Rev. B* **92**, 144426 (2015).
- [9] S. Chadov, J. Kiss, and C. Felser, *Adv. Func. Mater.* **23**, 832 (2013).
- [10] L. Wollmann, G. H. Fecher, S. Chadov, and C. Felser, *J. Phys. D: Appl. Phys.* **48**, 164004 (2015).
- [11] S. Chadov, S. W. D'Souza, L. Wollmann, J. Kiss, G. H. Fecher, and C. Felser, *Phys. Rev. B* **91**, 094203 (2015).
- [12] H. Chen, Q. Niu, and A. H. MacDonald, *Phys. Rev. Lett.* **112**, 017205 (2014).
- [13] W. H. Kleiner, *Phys. Rev.* **142**, 318 (1966).
- [14] M. Seemann, D. Ködderitzsch, S. Wimmer, and H. Ebert, *Phys. Rev. B* **92**, 155138 (2015).
- [15] J. C. Slater, *Phys. Rev.* **49**, 931 (1936).
- [16] L. Pauling, *Phys. Rev.* **54**, 899 (1938).
- [17] G. J. Li, E. K. Liu, Y. J. Zhang, Y. Du, H. W. Zhang, W. H. Wang, and G. H. Wu, *J. Appl. Phys.* **113**, 103903 (2013).
- [18] L. Wollmann, S. Chadov, J. Kübler, and C. Felser, *Phys. Rev. B* **92**, 064417 (2015).
- [19] A. K. Nayak, M. Nicklas, S. Chadov, P. Khuntia, C. Shekhar, A. Kalache, M. Baenitz, Y. Skourski, V. K. Guduru, A. Puri, et al., *Nat. Mater.* **14**, 679 (2015).
- [20] R. Stinshoff, A. K. Nayak, G. H. Fecher, B. Balke, S. Ouardi, Y. Skourski, T. Nakamura, and C. Felser, *Phys. Rev. B* **95**, 060410 (2017).
- [21] R. Stinshoff, G. H. Fecher, S. Chadov, A. K. Nayak, B. Balke, S. Ouardi, T. Nakamura, and C. Felser, accepted in *AIP Advances* (2017).
- [22] J. P. Perdew, K. Burke, and M. Ernzerhof, *Phys. Rev. Lett.* **77**, 3865 (1996).
- [23] H. Ebert, D. Ködderitzsch, and J. Minár, *Rep. Prog. Phys.* **74**, 096501 (2011).
- [24] D. Ködderitzsch, K. Chadova, and H. Ebert, *Phys. Rev. B* **92**, 184415 (2015).
- [25] P. Soven, *Phys. Rev.* **156**, 809 (1967).
- [26] D. W. Taylor, *Phys. Rev.* **156**, 1017 (1967).
- [27] H. Ebert, S. Mankovsky, K. Chadova, S. Polesya, J. Minár, and D. Ködderitzsch, *Phys. Rev. B* **91**, 165132 (2015).
- [28] K. Chadova, S. Mankovsky, J. Minár, and H. Ebert, *Phys. Rev. B* **95**, 125109 (2017).
- [29] S. Mankovsky, S. Polesya, K. Chadova, H. Ebert, J. B. Staunton, T. Gruenbaum, M. A. W. Schoen, C. H. Back, X. Z. Chen, and C. Song, *Phys. Rev. B* **95**, 155139 (2017).
- [30] V. N. Novogrudskii and I. G. Fakidov, *Sov. Phys. J.E.T.P.* **47**, 20 (1965).